POLITECNICO
MILANO 1863

SCUOLA DI INGEGNERIA INDUSTRIALE
E DELL'INFORMAZIONE

EXECUTIVE SUMMARY OF THE THESIS

A State Observer Design for a Direct-Drive Wind Energy Conversion System

LAUREA MAGISTRALE IN ELECTRICAL ENGINEERING - INGEGNERIA ELETTRICA

Author: MATTEO DEPONTI

Advisor: PROF. ROBERTO PERINI

Co-advisor: DR. DEJAN PEJOVSKI

Academic year: 2022-2023

1. Introduction

In recent years, renewable energy sources have come under increasing attention, mainly due to environmental concerns about global warming and de-carbonization policies. Among them, wind energy is becoming competitive with conventional sources of energy, with a cumulative installed capacity continuously increasing worldwide. In Wind Energy Conversion Systems (WECS), Permanent Magnet Synchronous Generators (PMSGs) are usually implemented in the so-called Type 4 configuration, where the generator is connected to the grid via a fully-rated power converter, constituting a Variable Frequency Drive (VFD).

In a drive system, the shaft's finite stiffness allows torsional oscillation between each rotating mass: if a torsional natural frequency is excited, a mechanical resonance condition occurs. Without a proper mitigation technique, torsional vibrations cause fatigue stress in the drive train and reliability issues.

Several methods to mitigate torsional vibrations can be found in the literature. Among them, PI-based State Space control enhances the capability of a PI control implementing a state observer, which is a mathematical model that, based on the available system measurements, provides an estimate of the system's state variables.

This thesis aims at designing a state observer for a two Degree-of-Freedom (DOF) drive system comprising a Permanent Magnet Synchronous Generator (PMSG) directly connected to a wind turbine. The mechanical and electrical models of the system are derived first. Two state observers will be proposed, each with its own formulation and performance analysis.

2. System Definition

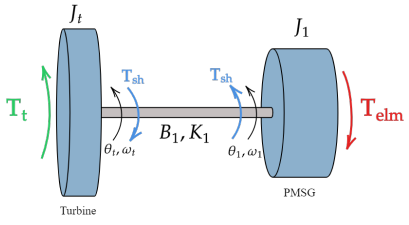

Figure 1: Two-Degree-of-Freedom (DOF) system sketch; subscript t stands for turbine, while 1 refers to the rotor of the PMSG

The two Degree-of-Freedom (DOF) system is outlined in Figure 1.

Table 1: PMSG and turbine parameters

PMSG and turbine parameters	
$P_n\ [MW]$; $T_n\ [Nm]$	1.0 ; $561{*}10^3$
$V_{n,ph}\ [V]$; $I_n\ [A]$	435 ; 713
$f_n\ [Hz]$; $\Psi_{PM}\ [Wb]$	14.73 ; 8.147
$poles\ (p)$; $n_p = \frac{p}{2}$	104 ; 52
$R_s\ [m\Omega]$; $L_s\ [m\dot{H}]$	14.59 ; 4.321
$D_{out,stator}\ [mm]$; $D_{out,rotor}\ [mm]$	5586 ; 5262
$K_{shaft} = K_1\ [\frac{Nm}{rad}]$	$1.2{*}10^{11}$
$J_{turbine} = J_t\ [kg\,m^2]$; $J_{rotor} = J_1\ [kg\,m^2]$	$3{*}10^6$; $3.36{*}10^6$

Neglecting the damping torque term, the equations of motion of the unforced mechanical system are:

$$\begin{cases} J_t\dot{\omega}_t + K_1(\theta_t - \theta_1) = 0 \\ J_1\dot{\omega}_1 - K_1(\theta_t - \theta_1) = 0 \end{cases} \tag{1}$$

By considering a simple harmonic motion as a solution of the two differential equations, the following system's natural frequencies can be found:

$$|f_{res}| = \left|\frac{\omega_{res}}{2\pi}\right| = \begin{bmatrix} 0 \\ 302.45 \end{bmatrix} [Hz] \tag{2}$$

The system mathematical model comprises the mechanical and electrical models in per unit (p.u.) form: the first one includes the equations of motion with the forcing terms, while the second one is defined by the dq stator voltage equations of the PMSG. Taking into consideration that:

- $\dot{\theta}_t = \omega_{b,mech}\omega_t$;
- $\dot{\theta}_1 = \omega_{b,mech}\omega_1$;
- the measurements of θ_1, i_{sd} and i_{sq} are available from the system, denoted with letter y;
- the damping torque term is neglected;

the system of differential equations can be defined through the following:

$$\begin{cases} \dot{\theta}_t = \omega_{b,mech}\omega_t \\ \dot{\theta}_1 = \omega_{b,mech}\omega_1 \\ \dot{\omega}_t = -\frac{K_1}{2H_tT_n}(\theta_t - \theta_1) + \frac{T_t}{2H_tT_n} \\ \dot{\omega}_1 = \frac{K_1}{2H_1T_n}(\theta_t - \theta_1) - \frac{T_{elm}}{2H_1T_n} \\ \dot{i_{sd}} = -r_s\frac{\omega_b}{l_s}i_{sd} + \omega_b i_{sq}\omega_1 + \frac{\omega_b}{l_s}v_{sd} \\ \dot{i_{sq}} = -r_s\frac{\omega_b}{l_s}i_{sq} - (\omega_b i_{sd} + \frac{\omega_b}{l_s}\psi_{PM})\omega_1 + \\ \quad + \frac{\omega_b}{l_s}v_{sq} \\ y_1 = \theta_1 \\ y_2 = i_{sd} \\ y_3 = i_{sq} \end{cases} \tag{3}$$

All the variables are expressed in p.u., so to have them of the same order of magnitude. Now, let us assume that the PMSG is fed by a 3-phase Voltage Source Converter (VSC) with Pulse Width Modulation (PWM) with:

- modulation frequency ratio: $m_f = \frac{f_{sw}}{f_c} = 33$ where:
  - f_{sw} is the switching frequency;
  - f_c is the carrier signal frequency;
- the VSC operates in linear modulation and produces only voltage harmonics of order:

  $$h_v = m\ m_f + n \mid m \in \mathbb{N}, n \in \mathbb{Z}$$

  where:
  - if m is even then n is odd;
  - if m is odd then n is even;
- the fundamental angular frequency of the stator voltage ω_{fund} corresponds to the rotor electrical angular frequency $\omega_{r,el}$:

  $$\omega_{fund} = \omega_{r,el} = \frac{p}{2}\omega_{r,mech}$$

  with $\omega_{r,mech}$ rotor mechanical angular frequency;

Based on [6], the torque harmonic of order h_T produced by the stator voltage harmonic component h_v is given by:

- $h_T = h_v - 1$ if $h_v = 6k + 1 \mid k \in \mathbb{N}$;
- $h_T = h_v + 1$ if $h_v = 6k - 1 \mid k \in \mathbb{N}$;
- no torque is produced if $h_v = 3k \mid k \in \mathbb{N}$;

In the Campbell diagram, the forcing terms' frequencies acting on the system, i.e. the torque harmonics' frequencies, are plotted together with the system's natural ones, in $[Hz]$, as a function of the machine rotating speed, usually in $[rpm]$. For this system, the diagram is shown in Figure 2.

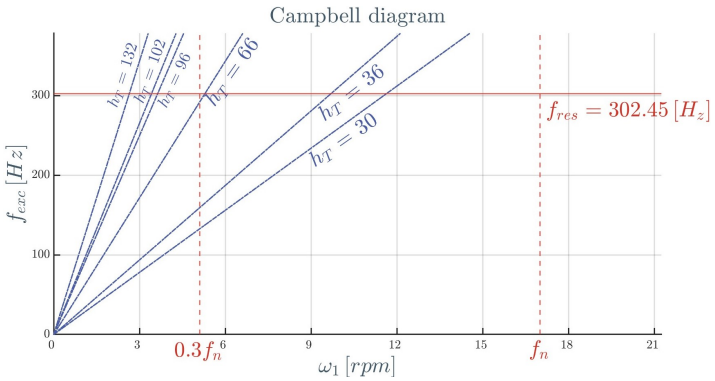

Figure 2: Campbell diagram showing the VSC produced torque harmonics which excite the resonance frequency of the system in the operating region

From the diagram is clear how the following voltage harmonic orders are able to generate a torque exciting the system's natural frequency in the operating region:

- $h_v = 31, 29 \rightarrow h_T = 30$;
- $h_v = 37, 35 \rightarrow h_T = 36$;
- $h_v = 67, 65 \rightarrow h_T = 66$;

3. Non-Linear Extended State Observer

In [3], a state observer for a Single-Input Single-Output (SISO) system in integral chain form with large uncertainty is defined, hence for a system of the kind:

$$\begin{cases} \dot{x}_1(t) = x_2(t); \\ \dot{x}_2(t) = x_3(t); \\ ... \\ \dot{x}_n(t) = f(t, x_1, x_2, ..., x_n) + w(t) + u(t); \\ y = x_1 \end{cases} \tag{4}$$

where $w(t) \in \mathbb{R}$ is an external disturbance and $f : \mathbb{R}^{n+1} \rightarrow \mathbb{R}$ a possibly unknown system function. Defining the extended state and its derivative as:

$$\begin{cases} x_{n+1}(t) = f(t, x_1, x_2, ..., x_n) + w(t); \\ \dot{x}_{n+1} = h(t) \end{cases} \tag{5}$$

and substituting (5) in (4), the following extended state system is obtained:

$$\begin{cases} \dot{x}_1(t) = x_2(t); \\ \dot{x}_2(t) = x_3(t); \\ ... \\ \dot{x}_n(t) = x_{n+1}(t) + u(t); \\ \dot{x}_{n+1} = h(t) \\ y = x_1 \end{cases} \tag{6}$$

Finally, the Extended State Observer (ESO) takes the form:

$$\begin{cases} \dot{\hat{x}}_1(t) = \hat{x}_2(t) - \alpha_1 g_1 \left(\hat{y}_1 - y_1\right); \\ \dot{\hat{x}}_2(t) = \hat{x}_3(t) - \alpha_2 g_2 \left(\hat{y}_1 - y_1\right); \\ ... \\ \dot{\hat{x}}_n(t) = \hat{x}_{n+1}(t) - \alpha_n g_n \left(\hat{y}_1 - y_1\right) + u(t); \\ \dot{\hat{x}}_{n+1} = -\alpha_{n+1} g_{n+1} \left(\hat{y}_1 - y_1\right) \\ \hat{y}_1 = \hat{x}_1 \end{cases} \tag{7}$$

where $\alpha_i \quad i = 1, ..., n, n+1$ are the observer gain coefficients and $g(.) : \mathbb{R} \rightarrow \mathbb{R}$ is a function that can be chosen linear or nonlinear: in the first case, the observer is called Linear Extended State Observer (LESO), while in the second case Non-Linear Extended State Observer (NLESO).

As can be seen in (3), in $\dot{i_{sd}}$ and $\dot{i_{sq}}$ equations two nonlinear terms appear:

- $\omega_b i_{sq} \omega_1$;
- $\omega_b i_{sd} \omega_1$.

Moreover, the NLESO is defined for a linear Single-Output system in integral chain form. The following operations are performed in order to obtain a system mathematical model suitable for an NLESO design:

- through a small perturbation approach, the system is linearized around the nominal working point;
- the Multi-Input Multi-Output (MIMO) system is divided into Multi-Input Single-Output (MISO) subsystems;
- an NLESO is designed for each subsystem and the final state variables' estimates are reconstructed through a relative-degree approach.

3.1. System Linearization

The generic state variable $x(t)$ can be split into the sum of a continuous steady-state term x_0 and an oscillating one (small perturbation) $\Delta x(t)$:

$$x(t) = x_0 + \Delta x(t) \tag{8}$$

Now, applying this concept to (3), splitting it with respect to the continuous and oscillating terms (Δ), isolating the latter one, and assuming that for a generic state variables x_i and x_j: $|\Delta x_i \Delta x_j| << |x_{i0} \Delta x_j| \mid i, j$, the following small perturbations (Δ) system is obtained:

$$\begin{cases} \Delta\dot{\theta}_t = \omega_{b,mech} \Delta\omega_t \\ \Delta\dot{\theta}_1 = \omega_{b,mech} \Delta\omega_1 \\ \Delta\dot{\omega}_t = -\frac{K_1}{2H_t T_n} \left(\Delta\theta_t - \Delta\theta_1\right) \\ \Delta\dot{\omega}_1 = \frac{K_1}{2H_1 T_n} \left(\Delta\theta_t - \Delta\theta_1\right) - \\ \quad - \frac{n_p (I_b \psi_b) \psi_{PM}}{2H_1 T_n} \Delta i_{sq} \\ \Delta\dot{i}_{sd} = -r_s \frac{\omega_b}{l_s} \Delta i_{sd} + \omega_b \omega_{10} \Delta i_{sq} + \\ \quad + \omega_b i_{sq0} \Delta\omega_1 + \frac{\omega_b}{l_s} \Delta v_{sd} \\ \Delta\dot{i}_{sq} = -r_s \frac{\omega_b}{l_s} \Delta i_{sq} - \omega_b \omega_{10} \Delta i_{sd} + \\ \quad - \frac{\omega_b}{l_s} \psi_{PM} \Delta\omega_1 + \frac{\omega_b}{l_s} \Delta v_{sq} \\ \Delta y_1 = \Delta\theta_1 \\ \Delta y_2 = \Delta i_{sd} \\ \Delta y_3 = \Delta \mathrm{i_{sq}} \end{cases} \tag{9}$$

It must be noticed that:

- $\omega_{10} = \frac{\omega_{n,mech}}{\omega_{b,mech}}$;
- $i_{sd0} = 0$ (Max. Torque per Ampere);
- $i_{sq0} = \frac{T_{elm,0}}{n_p(I_b\psi_b)\psi_{PM}}$;

System (9) can be represented in matrix form:

$$\begin{aligned}\dot{\mathbf{\Delta x}} &= \mathbf{\Delta A \Delta x} + \mathbf{\Delta B \Delta u} \\ \mathbf{\Delta y} &= \mathbf{\Delta C \Delta x}\end{aligned}$$

where:

$$\mathbf{\Delta x} = \begin{bmatrix} \Delta\theta_t \\ \Delta\theta_1 \\ \Delta\omega_t \\ \Delta\omega_1 \\ \Delta i_{sd} \\ \Delta i_{sq} \end{bmatrix}; \quad \mathbf{\Delta u} = \begin{bmatrix} \Delta v_{sd} \\ \Delta v_{sq} \end{bmatrix}; \quad \mathbf{\Delta y} = \begin{bmatrix} \Delta\theta_1 \\ \Delta i_{sd} \\ \Delta i_{sq} \end{bmatrix}.$$

3.2. Subsystem Decomposition

In the form shown in (9), the system is in a Multi-Input Multi-Output (MIMO) form. To design an NLESO, the system is decomposed in three different Multi-Input Single-Output (MISO) subsystems; the procedure can be summarized as follows:

1. create three identical subsystems, each one defined by one of the three outputs in $\mathbf{\Delta y}$ of system (9)
   - in this way three subsystems are obtained, in the form:

$$\begin{aligned}\dot{\mathbf{\Delta x}} &= \mathbf{\Delta A \Delta x} + \mathbf{\Delta B \Delta u} \\ \Delta y_i &= \mathbf{\Delta C}_i \mathbf{\Delta x}\end{aligned} \quad | \; i = 1, 2, 3 \; ;$$

2. check that each pair $(\mathbf{\Delta C}_i \, , \mathbf{\Delta A})$ is observable [1], which is a necessary condition for the state observer realization:
   - if not, find the non-observable state variables applying the kernel to the Observability Matrix [2] and reshape the subsystem of interest's matrices accordingly;
   - verify that the newfound subsystem is observable;
3. define the subsystems' final shape in matrix form:

$$\begin{aligned}\dot{\mathbf{\Delta x}}_i &= \mathbf{\Delta A}_i \mathbf{\Delta x}_i + \mathbf{\Delta B}_i \mathbf{\Delta u} \\ \Delta y_i &= \mathbf{\Delta C}_i \mathbf{\Delta x}_i\end{aligned} \quad | \; i = 1, 2, 3 \; ;$$

Finally, the three MISO subsystems' state variables and output are:

Subsystem 1

$$\mathbf{\Delta x}_1 = \mathbf{\Delta x}; \quad \Delta y_1 = \Delta\theta_1 \; ;$$

Subsystem 2 and 3

$$\mathbf{\Delta x}_2 = \mathbf{\Delta x}_3 = \begin{bmatrix} \Delta\theta_t - \Delta\theta_1 \\ \Delta\omega_t \\ \Delta\omega_1 \\ \Delta i_{sd} \\ \Delta i_{sq} \end{bmatrix}; \quad \begin{aligned} \Delta y_2 &= \Delta i_{sd} \; ; \\ \Delta y_3 &= \Delta i_{sq} \; ; \end{aligned}$$

3.3. Relative Degree Analysis

In [7], a systematic procedure for distributed state estimation in nonlinear systems is presented. Particularly, a relative degree analysis, with which the closeness between states and outputs can be evaluated, is provided. Based on this analysis, it is assumed that the closer the state to the output used as the observer input, the more accurate the estimation of the state variable.
A generic MISO system can be expressed in the form:

$$\begin{cases} \dot{\mathbf{x}} = \mathbf{f}(\mathbf{x}) + \mathbf{g}(\mathbf{u}) \\ y = \mathbf{h}(\mathbf{x}) \end{cases} \tag{10}$$

Let us start defining matrix $\mathbf{F}$ as:

$$\mathbf{F} = \frac{\partial \mathbf{f}}{\partial \mathbf{x}} = [\; \mathbf{F_1} \quad \mathbf{F_2} \quad ... \quad \mathbf{F_n} \;] \tag{11}$$

where $\mathbf{F_i} \mid i = 1, ..., n$ are column vectors.
Another useful concept to be introduced is the Lie derivative [4] of $\mathbf{h}(\mathbf{x})$ along $\mathbf{F_i} \mid i = 1, ..., n$, defined as:

$$L_{\mathbf{F_i}} \mathbf{h}(\mathbf{x}) \triangleq \frac{\partial \mathbf{h}(\mathbf{x})}{\partial \mathbf{x}} * \mathbf{F_i}(\mathbf{x}) \tag{12}$$

The closeness between the output y and the generic subsystem variable $x_i \in \mathbf{x} \mid i = 1, ..., n$ is evaluated by calculating D_i:

$$D_i = \begin{cases} 0 \quad \text{if} \quad \frac{\partial \mathbf{h}}{\partial x_i} \neq 0 \\ 1 \quad \text{if} \quad \begin{cases} \frac{\partial \mathbf{h}}{\partial x_i} = 0 \\ L_{\mathbf{F_i}} \mathbf{h}(\mathbf{x}) \neq 0 \end{cases} \\ d_i \quad \text{if} \quad \begin{cases} \frac{\partial \mathbf{h}}{\partial x_i} = 0 \\ L_{\mathbf{F_i}} L_{\mathbf{f}}^{k-1} \mathbf{h}(\mathbf{x}) = 0 \mid k = 0, 1, ..., d_i - 1 \\ L_{\mathbf{F_i}} L_{\mathbf{f}}^{d_i - 1} \mathbf{h}(\mathbf{x}) \neq 0 \end{cases} \\ \infty \quad \text{if} \quad d_i \to \infty \end{cases}$$

The lower D_i the closer is the state variable $x_i \mid i = 1, ..., n$ to the output y.
This analysis is applied to each subsystem; the different values of D_i can be found in Table 2.

Table 2: Relative degrees between the state variables and each subsystem's output

Subsystem 1 $i = 1, ..., n_1$		Subsystem 2 $i = 1, ..., n_2$		Subsystem 3 $i = 1, ..., n_3$	
$\mathbf{\Delta x_1}$	D_{1i}	$\mathbf{\Delta x_2}$	D_{2i}	$\mathbf{\Delta x_3}$	D_{3i}
$\Delta\theta_t$	2	$\Delta\theta_t - \Delta\theta_1$	2	$\Delta\theta_t - \Delta\theta_1$	2
$\Delta\theta_1$	0				
$\Delta\omega_t$	3	$\Delta\omega_t$	3	$\Delta\omega_t$	3
$\Delta\omega_1$	1	$\Delta\omega_1$	1	$\Delta\omega_1$	1
Δi_{sd}	3	Δi_{sd}	0	Δi_{sd}	1
Δi_{sq}	2	Δi_{sq}	1	Δi_{sq}	0

The overall procedure is summarized in the block scheme of Figure 3.

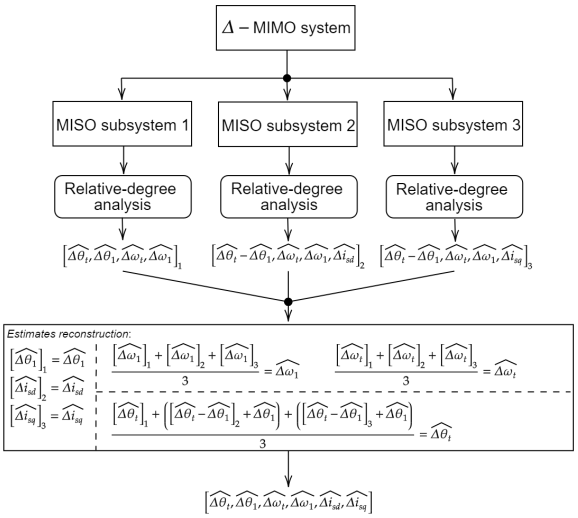

Figure 3: simple block scheme of the steps taken from subsystem decomposition to estimates reconstruction.

3.4. NLESO definition

An NLESO has to be defined for each subsystem. A requirement is to have a system in integral chain form, thus a state variable transformation is needed, that is to find an invertible matrix $\mathbf{T}_i \mid i = 1, 2, 3$ for each subsystem such that:

$$\mathbf{z}_i = \mathbf{T}_i \mathbf{\Delta x}_i \tag{13}$$

The three transformed MISO subsystems take the form:

$$\begin{aligned} \mathbf{z_i} &= \mathbf{A_{zi} z_i} + \mathbf{B_{zi}} \mathbf{\Delta u} \\ y_i &= \mathbf{C_{zi} z_i} \end{aligned} \quad \mid i = 1, 2, 3$$

Now, considering:

- number of inputs: $p = 2$;
- $$\mathbf{B_z} = \begin{bmatrix} B_{z11} & B_{z12} \\ B_{z21} & B_{z22} \\ ... & ... \\ B_{zn1} & B_{zn2} \end{bmatrix};$$

each MISO transformed subsystem takes the form:

$$\begin{cases} \dot{z_1} = z_2 + B_{z11} u_1 + B_{z12} u_2; \\ \dot{z_2} = z_3 + B_{z21} u_1 + B_{z22} u_2; \\ ... \\ \dot{z_n} = f(z_1, ..., z_n) + B_{zn1} u_1 + B_{zn2} u_2; \\ y = z_1 \end{cases} \tag{14}$$

where $n = 6$ for Subsystem 1 and $n = 5$ for Subsystems 2 and 3. Following the definition of extended state in (5), an NLESO can be designed:

$$\begin{cases} \dot{\widehat{z_1}} = \widehat{z_2} + B_{z11} u_1 + B_{z12} u_2 - \\ \quad -\beta_1 g(\widehat{y} - y); \\ \dot{\widehat{z_2}} = \widehat{z_3} + B_{z11} u_1 + B_{z12} u_2 - \\ \quad -\beta_2 g(\widehat{y} - y); \\ ... \\ \dot{\widehat{z_n}} = \widehat{z_{n+1}} + B_{z11} u_1 + B_{z12} u_2 - \\ \quad -\beta_n g(\widehat{y} - y); \\ \dot{\widehat{z_{n+1}}} = \widehat{h} - g(\widehat{y} - y); \\ \widehat{y} = \widehat{z_1} \end{cases} \tag{15}$$

where the $\hat{z}_i$ represents the state estimations and β_i are the observer gain coefficients, with $i = 1, ..., n, n+1$.
The observer correction term is chosen as the product between the β coefficients and the nonlinear function $g(e_1) \mid e_1 = \widehat{y} - y$:

$$g(e_1) = \begin{cases} \frac{e_1}{\delta^{1-\alpha}} & |e_1| \leq \delta \\ |e_1|^\alpha \operatorname{sign}(e_1) & |e_1| > \delta \end{cases} \quad \mid \alpha, \delta \in \mathbb{R}^+$$

By taking the difference between $\mathbf{z} - \widehat{\mathbf{z}}$, the observation error system is obtained:

$$\begin{cases} \dot{e_1} = e_2 - \beta_1 g(e_1) \\ \dot{e_2} = e_3 - \beta_2 g(e_1) \\ \dot{e_n} = e_{n+1} - \beta_n g(e_1) \\ \dot{e_{n+1}} = (\widehat{h} - h) - \beta_{n+1} g(e_1) \\ \hat{y} - y = e_1 \end{cases} \tag{16}$$

Now, defining $\Gamma(e_1) = g(e_1) - e_1$, (16) can rewritten as::

$$\begin{cases} \dot{e_1} = e_2 - \beta_1 e_1 + \beta_1 (-\Gamma(e_1)) \\ \dot{e_2} = e_3 - \beta_2 e_1 + \beta_2 (-\Gamma(e_1)) \\ \dots \\ \dot{e_n} = e_{n+1} - \beta_n e_1 + \beta_n (-\Gamma(e_1)) \\ e_{n+1} = (\hat{h} - h) - \beta_{n+1} e_1 + \\ \quad +\beta_{n+1} (-\Gamma(e_1)) \\ \hat{y} - y = e_1 \end{cases} \tag{17}$$

Finally, if:

- $\Gamma(e_1)$ is a Lipschitz nonlinearity that satisfies a sector condition;
- the β-coefficients for each MISO subsystem's observer are chosen such that:
  - $(\mathbf{A_e}, \mathbf{B_e})$ controllable:
  - $(\mathbf{C_e}, \mathbf{A_e})$ observable;

the observation error system represents a Lur'e problem and absolute stability can be guaranteed by applying the circle criterion [4].

3.5. Simulation Results

The main objective of the simulation is to assess the estimation performance of the state observer when the mechanical system is subject to torsional vibrations. For this reason, the simulation analysis is divided into three steps:

1. operation in ideal conditions, i.e. no voltage harmonic injection;
2. operation in perturbed conditions through the injection of a voltage harmonic at a frequency f_{dist} far from the system's natural frequency;
3. operation in perturbed conditions through the injection of a voltage harmonic at a frequency f_{res} that excites the system's natural frequency;

The turbine and PMSG rotor angular speed trends and the reference ω_{ref} are displayed in Figure 4.

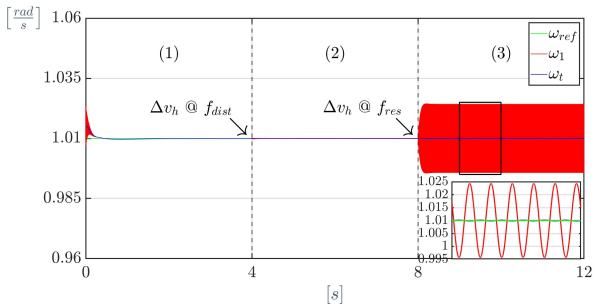

Figure 4: Simulation speeds' trends

The plots regarding the angular position $\Delta\theta_t$ and $\Delta\theta_1$ are shown in Figure 5 and 6.

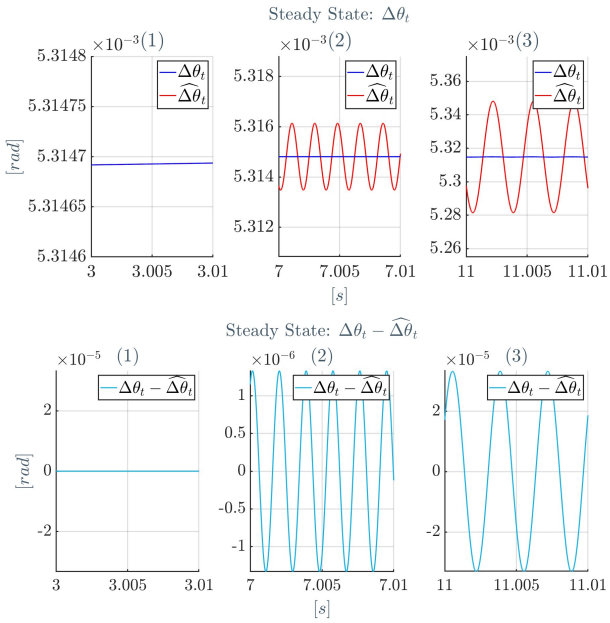

Figure 5: $\Delta\theta_t$ true value and estimate comparison (top) and observation error $e_1 = \Delta\theta_t - \widehat{\Delta\theta_t}$ (bottom) at steady state

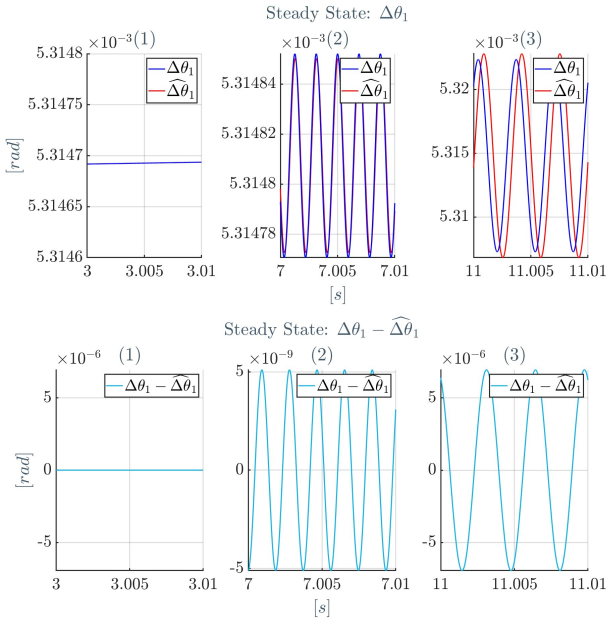

Figure 6: $\Delta\theta_1$ true value and estimate comparison (top) and observation error $e_2 = \Delta\theta_1 - \widehat{\Delta\theta_1}$ (bottom) at steady state

The estimation for $\Delta\theta_t$ provided by the NLESO is characterized by a relatively big estimation error: the estimated variable has strong oscillations which are not present in the real value. On the other hand, the estimation of $\Delta\theta_1$ appears to be more accurate, probably because this state variable is Subsystem 1's observer in-

put.
Some final considerations can be made about the NLESO. First of all, the state observer is stable. Moreover, the NLESO provides the most accurate estimates for the state variables that are also the subsystems' observers' inputs. On the other hand, the NLESO's estimation performance is highly influenced by the presence of disturbances, as it is shown by the high observation errors when a voltage harmonic is injected. Moreover, the state observer design is quite cumbersome and the computational burden required to estimate several state variables for three different subsystems can be considered another limiting factor.

4. Luenberger-based Lipschitz Observer

By isolating the nonlinear terms present in (3), i.e. define a nonlinear function $\mathbf{\Phi}(\mathbf{x},t)$, and rewriting the same system in matrix form, the following representation is obtained:

$$\begin{aligned}\dot{\mathbf{x}} &= \mathbf{A}\mathbf{x} + \mathbf{\Phi}(\mathbf{x},t) + \mathbf{B}\mathbf{u} \\ \mathbf{y} &= \mathbf{C}\mathbf{x}\end{aligned} \tag{18}$$

$$\mathbf{x} = \begin{bmatrix} \theta_t \\ \theta_1 \\ \omega_t \\ \omega_1 \\ i_{sd} \\ i_{sq} \end{bmatrix}; \quad \mathbf{u} = \begin{bmatrix} T_t \\ v_{sd} \\ v_{sq} \end{bmatrix}; \quad \mathbf{y} = \begin{bmatrix} \theta_1 \\ i_{sd} \\ i_{sq} \end{bmatrix}; \quad \mathbf{\Phi}(\mathbf{x}) = \begin{bmatrix} 0 \\ 0 \\ 0 \\ 0 \\ \omega_b i_{sq} \omega_1 \\ -\omega_b i_{sd} \omega_1 \end{bmatrix}.$$

Under the hypothesis that:

- $\mathbf{\Phi}(\mathbf{x},t)$ is a Lipschitz function with Lipschitz constant γ;
- the pair $(\mathbf{C},\mathbf{A})$ is observable.

a Luenberger state observer can be defined as [5]:

$$\begin{aligned}\dot{\hat{\mathbf{x}}} &= \mathbf{A}\hat{\mathbf{x}} + \mathbf{B}\mathbf{u} + \mathbf{\Phi}(\hat{\mathbf{x}},t) + \mathbf{L}\mathbf{C}\left(\mathbf{x} - \hat{\mathbf{x}}\right) \\ \hat{\mathbf{y}} &= \mathbf{C}\hat{\mathbf{x}}\end{aligned} \tag{19}$$

where $\mathbf{L}$ is the observer gain matrix, to be found solving the Lyapunov equation for $\mathbf{P} = \mathbf{P}^T > 0$:

$$\left[\mathbf{A}^T + \beta\mathbf{I}\right]\mathbf{P} + \mathbf{P}\left[\mathbf{A}^T + \beta\mathbf{I}\right]^T = -2\mathbf{C}^T\mathbf{C}$$

where β is a constant satisfying:

$$\beta > \gamma$$

and finally computing:

$$\mathbf{L} = \mathbf{P}^{-1}\mathbf{C}^T$$

For system (18):

- $\gamma = 189.80 \rightarrow \beta = 190$;
-

$$\mathbf{L} = \begin{bmatrix} 190.03 & 0 & -2.65 \\ 190.09 & 0 & -7.01 \\ 5.97 & 0 & -488.12 \\ 36.85 & 0 & -2990.41 \\ 0 & 186.62 & 0 \\ -7.01 & 0 & 756.54 \end{bmatrix}.$$

4.1. Observation Error BIBO stability

In [5] there is no detailed demonstration to prove the observation error stability in case of the simple condition $\beta > \gamma$: therefore, a deeper analysis is needed to assess whether the system is at least Bounded Input Bounded Output (BIBO) stable. In this way, it is possible to check if the observer has an unstable behavior due to the nonlinear terms.
Subtracting (19) from (18), the observation error system dynamic system is obtained:

$$\begin{aligned}\dot{\mathbf{e}} &= \dot{\mathbf{x}} - \dot{\hat{\mathbf{x}}} = \\ &= \left(\mathbf{A} - \mathbf{L}\mathbf{C}\right)\mathbf{e} + \left[\mathbf{\Phi}(\mathbf{x},t) - \mathbf{\Phi}(\hat{\mathbf{x}},t)\right] \\ &= \mathbf{A}_\mathbf{e}\mathbf{e} + \mathbf{\Phi}_\mathbf{e}(\hat{\mathbf{x}},\mathbf{x},t)\end{aligned}$$

By looking at the nonlinear term $\mathbf{\Phi}_\mathbf{e}(\hat{\mathbf{x}},\mathbf{x},t)$ as an input disturbance, it can be seen as:

$$\begin{aligned}\mathbf{\Phi}_\mathbf{e}(\hat{\mathbf{x}},\mathbf{x},t) &= \begin{bmatrix} 0 \\ 0 \\ 0 \\ 0 \\ \omega_b i_{sq}\omega_1 - \omega_b \widehat{i_{sq}\omega_1} \\ -\omega_b i_{sd}\omega_1 + \omega_b \widehat{i_{sd}\omega_1} \end{bmatrix} = \\ &= \mathbf{B}_{\mathbf{\Phi}_\mathbf{e}}\mathbf{u}_{\mathbf{\Phi}_\mathbf{e}} = \begin{bmatrix} 0 & 0 \\ 0 & 0 \\ 0 & 0 \\ 0 & 0 \\ \omega_b & 0 \\ 0 & \omega_b \end{bmatrix} \begin{bmatrix} i_{sq}\omega_1 - \widehat{i_{sq}\omega_1} \\ -i_{sd}\omega_1 + \widehat{i_{sd}\omega_1} \end{bmatrix}\end{aligned} \tag{20}$$

The observation error transfer function is defined as:

$$\mathbf{G}_\mathbf{e}(s) = \frac{\mathbf{e}(s)}{\mathbf{u}_{\mathbf{\Phi}_\mathbf{e}}(s)} = \left(s\mathbf{I} - \mathbf{A}_\mathbf{e}\right)^{-1}\mathbf{B}_{\mathbf{\Phi}_\mathbf{e}} \tag{21}$$

Now, recalling the Bounded Input Bounded Output (BIBO) stability property of a system [2] , the observation error dynamics system is BIBO stable if a bounded input $\mathbf{u}_{\mathbf{\Phi}_\mathbf{e}}$ leads to a bounded output $\mathbf{y}_\mathbf{e} = \mathbf{e}$. Considering that:

- the input $\mathbf{u_{\Phi_e}}$ consists of the subtraction of the same Lipschitz function operating with two different variables, i.e. $\mathbf{x}$ and $\widehat{\mathbf{x}}$, which belong to a bounded domain given by the operating region of the system;
- $\lim_{\widehat{\mathbf{x}}\to\mathbf{x}} \mathbf{u_{\Phi_e}} = \lim_{\widehat{\mathbf{x}}\to\mathbf{x}} \mathbf{\Phi_e}\left(\mathbf{x}, \widehat{\mathbf{x}}\right) \to 0$;
- the magnitude of each element of $\mathbf{G_e}(s)$ is bounded in the frequency domain;

the observation error dynamics system can be assumed BIBO stable.

4.2. Simulation results

To properly compare the two state observers defined in this thesis, the two simulation setups are kept the same: in this way, each observer is tested under the same operating conditions.

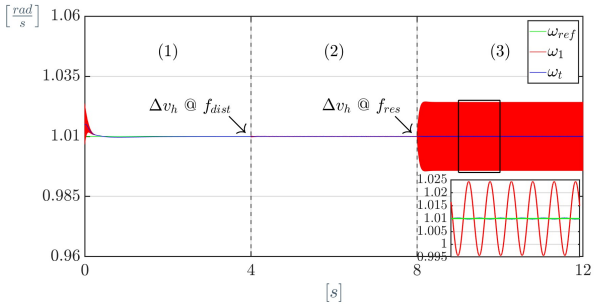

Figure 7: Speeds used in the simulation

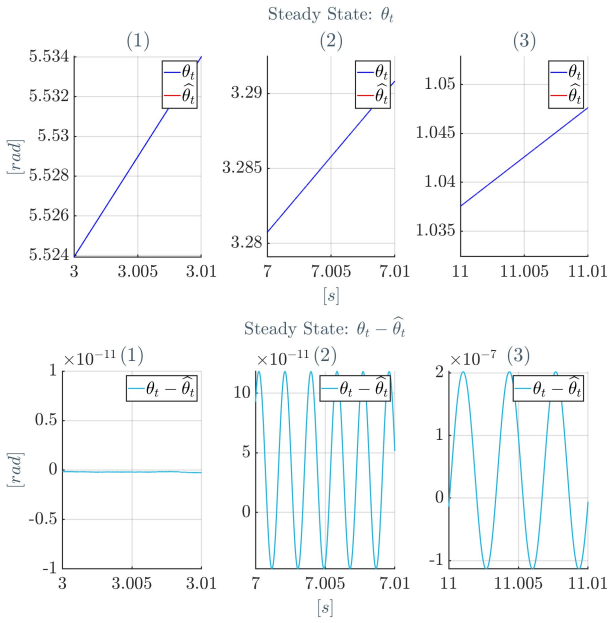

Figure 8: θ_t true value and estimate comparison (top) and observation error $e_1 = \theta_t - \widehat{\theta}_t$ (bottom) at steady state

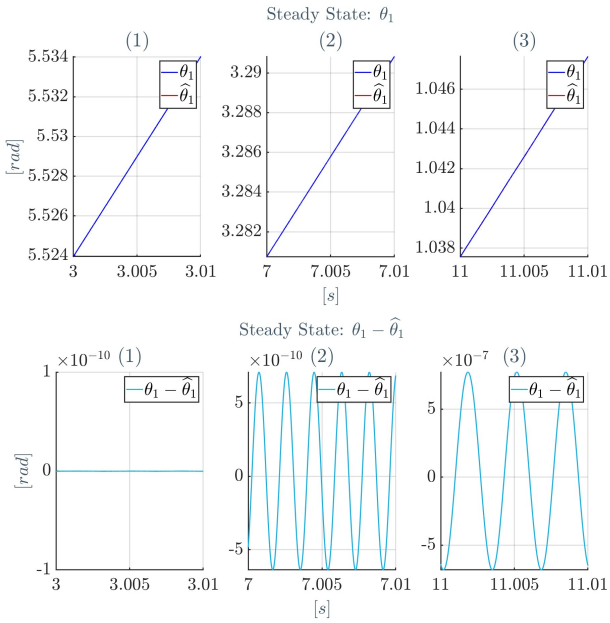

Figure 9: θ_1 true value and estimate comparison (top) and observation error $e_2 = \theta_1 - \widehat{\theta}_1$ (bottom) at steady state

The angular positions θ_t and θ_1's graphs are shown in Figure 8 and 9: the observation error for both the state variables θ_t and θ_1 tends quickly to a small value that oscillates around zero. The worst estimation is given during the mechanical resonance phenomenon, with a small error at steady state.
Based on the simulation results, some final remarks can be made. Also in this case the state observer is stable, but now more accurate estimates are provided for all the state variables compared to the NLESO case. The observer performance decreases during mechanical resonance conditions, while it is less affected by a generic disturbance such as the voltage harmonic injection at frequency f_{dist}. In this case, the state observer design is much easier than the NLESO and it deals with the nonlinear MIMO system. Further analysis regarding the observer's stability is required.

5. Conclusions

A two Degree-of-Freedom (DOF), comprising a Permanent Magnet Synchronous Generator (PMSG) directly connected to a Wind Turbine, was considered. Two different state observers were presented, considering as measured variables only the PMSG rotor position and the stator current's direct and quadrature compo-

nents. When considering the electrical model of the system, some nonlinear terms appear.
First, a Non-Linear Extended State Observer (NLESO) working on a linearized model of the system was proposed. The results can be summarized as follows:

- the design of this observer type appears to be quite complex and cumbersome, although it was possible to prove the absolute stability of the observation error;
- the estimates have a low level of accuracy, especially during torsional vibrations.

Then, a Luenberger-based Lipschitz Observer was proposed:

- its design is less complex than the previous observer and it deals directly with the nonlinear system. Further investigation regarding its stability is required;
- the observer can provide accurate estimates of all the state variables and it is more robust to generic disturbances.

6. Acknowledgements

I want to express my deep gratitude to Prof. Roberto Perini and Dr. Dejan Pejovski, not only for the precious technical support and motivation but also for teaching me how to encourage others and how to value their work: I sincerely believe that this thesis has helped me grow both as a person and an engineer.

References

[1] P. Bolzern, R. Scattolini, and N. Schiavoni. *Fondamenti di controlli automatici*. Collana di istruzione scientifica. McGraw-Hill Companies, 2008.

[2] O.M. Grasselli, L. Menini, and S. Galeani. *Sistemi dinamici*. Hoepli, 2007.

[3] Bao-Zhu Guo and Zhiliang Zhao. *Active Disturbance Rejection Control for Nonlinear Systems: An Introduction*. 10 2016.

[4] H.K. Khalil. *Nonlinear Systems*. Pearson Education. Prentice Hall, 2002.

[5] Panos C. Papageorgiou and Antonio T. Alexandridis. A direct pole placement-based approach for the design of nonlinear lipschitz observers. In *2020 European Control Conference (ECC)*, pages 1520–1525, 2020.

[6] Joseph Song-Manguelle, Gabriel Ekemb, Stefan Schröder, Tobias Geyer, Jean-Maurice Nyobe-Yome, and Rene Wamkeue. Analytical expression of pulsating torque harmonics due to pwm drives. In *2013 IEEE Energy Conversion Congress and Exposition*, pages 2813–2820, 2013.

[7] Xunyuan Yin, Kevin Arulmaran, and Jinfeng Liu. Subsystem decomposition for distributed state estimation of nonlinear systems. pages 5569–5574, 2016.